Preclinical Efficacy of the c-Met Inhibitor CE-355621 in a U87 MG Mouse Xenograft Model Evaluated by ^{18}F-FDG Small-Animal PET

Jeffrey R. Tseng*[1], Keon Wook Kang*[2], Mangal Dandekar[1], Shahriar Yaghoubi[1], Joseph H. Lee[3], James G. Christensen[3], Stephen Muir[4], Patrick W. Vincent[5], Neil R. Michaud[5], and Sanjiv S. Gambhir[1,6]

[1]*Molecular Imaging Program at Stanford, Bio-X Program, and Department of Radiology, Stanford University, Stanford, California;* [2]*Department of Nuclear Medicine, National Cancer Center, Goyang, South Korea;* [3]*Cancer Biology, PGRD-La Jolla Laboratories, Pfizer Inc., La Jolla, California;* [4]*Oncology, PGRD-New London, Pfizer, Inc., New London, Connecticut;* [5]*Cancer Biology, PGRD-Groton Laboratories, Pfizer Inc., Groton, Connecticut; and* [6]*Department of Bioengineering, Stanford University, Stanford, California*

The purpose of this study was to evaluate the efficacy of CE-355621, a novel antibody against c-Met, in a subcutaneous U87 MG xenograft mouse model using ^{18}F-FDG small-animal PET. **Methods:** CE-355621 or control vehicle was administered intraperitoneally into nude mice (drug-treated group, $n = 12$; control group, $n = 14$) with U87 MG subcutaneous tumor xenografts. Drug efficacy was evaluated over 2 wk using ^{18}F-FDG small-animal PET and compared with tumor volume growth curves. **Results:** The maximum %ID/g (percentage injected dose per gram of tissue) of ^{18}F-FDG accumulation in mice treated with CE-355621 remained essentially unchanged over 2 wk, whereas the %ID/g of the control tumors increased 66% compared with the baseline. Significant inhibition of ^{18}F-FDG accumulation was seen 3 d after drug treatment, which was earlier than the inhibition of tumor volume growth seen at 7 d after drug treatment. **Conclusion:** CE-355621 is an efficacious novel antineoplastic chemotherapeutic agent that inhibits ^{18}F-FDG accumulation earlier than tumor volume changes in a mouse xenograft model. These results support the use of ^{18}F-FDG PET to assess early tumor response for CE-355621.

Key Words: CE-355621; c-Met inhibitor; ^{18}F-FDG; microPET; drug evaluation; therapy response

J Nucl Med 2008; 49:129–134
DOI: 10.2967/jnumed.106.038836

CE-355621 is a novel monoclonal antibody that binds to the extracellular domain of c-Met (*1*). c-Met is a receptor tyrosine kinase involved in multiple pathways linked to cancer—such as cell migration, invasion, proliferation, and angiogenesis—and is upregulated in a large number of human cancers (*2,3*). This novel antibody may serve as an antineoplastic chemotherapeutic by disrupting several of these pathways. Tumor growth has been inhibited in several tumor xenograft models in which the antibody blocks autocrine activation of c-Met from hepatocyte growth factor (HGF) released from the tumors (*1*).

^{18}F-FDG PET has been validated as an imaging modality to assess a wide range of cancers for a wide range of indications—including diagnosis, staging, and restaging—and to assess response to therapy (*4*). With the development of microPET scanners for small animals (*5*), assessment of tumor xenograft mouse models with ^{18}F-FDG became possible for preclinical oncology research. Several authors have used ^{18}F-FDG microPET to assess various therapies in mouse tumor xenograft models (*6–9*). In addition, several studies have compared ^{18}F-FDG microPET with an alternative proliferation tracer, 3′-deoxy-3′-^{18}F-fluorothymidine (^{18}F-FLT), to assess tumor xenograft response to a variety of therapies (*10–13*). We have recently shown that microPET studies are reproducible with moderately low variability, such that serial studies on mouse tumor xenografts can be reliable in assessing therapy response (*14,15*).

This study was performed to assess the preclinical efficacy of CE-355621 to inhibit ^{18}F-FDG accumulation in vivo using a U87 MG human glioblastoma mouse xenograft tumor model. We show that CE-355621 inhibits ^{18}F-FDG accumulation earlier than changes in tumor volume, which supports the use of ^{18}F-FDG PET in human clinical trials for early therapy monitoring. These preclinical ^{18}F-FDG PET results may be useful to predict the success of future human clinical trials and may prove useful in accelerating drug development.

MATERIALS AND METHODS

Drug

CE-355621 (Pfizer Inc.) is a monoclonal antibody antagonist that binds to the extracellular domain of the c-Met tyrosine kinase. A stock solution of 10 mg/mL CE-355621 was stored in a solution

Received Dec. 15, 2006; revision accepted Sep. 18, 2007.
For correspondence or reprints contact: Sanjiv S. Gambhir, MD, PhD, Molecular Imaging Program at Stanford (MIPS), Division of Nuclear Medicine, Departments of Radiology and Bioengineering, Bio-X Program; The James H. Clark Center, 318 Campus Dr., East Wing, 1st Floor, Stanford, California 94305-5427.
E-mail: sgambhir@stanford.edu
*Contributed equally to this work.

of 20 mM sodium acetate, pH 5.5, and 140 mM sodium chloride at 4°C. Before use, the drug was dissolved in phosphate-buffered saline to a final concentration of 1 μg/μL.

Cell Culture

U87 MG human glioblastoma cells (*16*) were grown in Dulbecco's modified Eagle media, supplemented with 10% fetal bovine serum (Invitrogen). Cells were grown in T-225 flasks at 37°C with 5% carbon dioxide in a humidified incubator. Cells were harvested or split at approximately 90% confluence by trypsinization. For implantation into nude mice, cells were resuspended in phosphate-buffered saline and incubated on ice until injection.

Mouse Xenograft Model

Animal protocols were approved by the Stanford Administrative Panel on Laboratory Animal Care. Forty-five 8-wk-old female nude (*nu/nu*) mice (Charles River Laboratories) were injected subcutaneously with 1×10^6 U87 MG cells in the right flank while anesthetized with 2% isoflurane in 1 L of oxygen. Mice were weighed and tumors were measured with external calipers every 2–3 d. Tumor volumes were estimated as length × width × width ÷ 2. After 6 d, when tumors reached an approximate volume of 200 mm^3, 32 mice were selected for further study. During the study, 5 animals died while they were in the anesthesia chamber; the deaths were likely due to hypothermia from a malfunctioning heating pad. One mouse in the drug-treated group was excluded, as no drug was detected in the blood at the end of the study. The final count consisted of 12 mice in the drug-treated group and 14 mice in the control group.

^{18}F-FDG microPET

The drug dosing and imaging schedules were as follows. Mice were administered one dose of 200 μg CE-355621 (in a total volume of 200 μL) or the control vehicle saline solution by intraperitoneal injection on day 7 after tumor cell inoculation. On day 6, a baseline microPET scan was performed before the drug dose, followed by imaging on days 8, 10, 14, and 16. The control arm of the study was stopped after day 16 because the tumor burden was >10% of the body weight, which was the euthanasia criterion in the animal protocol. Monitoring of the drug-treated arm was continued, and a final scan was obtained on day 21.

Before imaging, mice were fasted for 4 h and had free access to water. Approximately 7.4 MBq (200 μCi) of ^{18}F-FDG (Siemens/PETNET) were injected via the tail vein. Tail vein blood glucose levels were recorded after injection. One hour after injection, mice were scanned prone in a microPET R4 (Siemens Medical Solutions, Inc.). The scanner has an approximate spatial resolution of 2 mm in each orthogonal direction (*17*), which was confirmed by phantom studies in our laboratory. Mice were maintained under isoflurane anesthesia and on a heating pad during the injection, uptake period, and scan. Rectal temperatures were recorded periodically to monitor physiologic body temperatures while under anesthesia. A 5-min static acquisition was performed with no attenuation correction, as described previously (*14*). Images were reconstructed using a 2-dimensional ordered-subsets expectation maximization algorithm (*18*) with 16 subsets and 4 iterations. A sample 3-dimensional rendering of an ^{18}F-FDG microPET scan is included in Supplemental Video 1 (supplemental material is available online only at http://jnm.snmjournals.org).

microPET Image Analysis

Ellipsoidal regions of interest (ROIs) were drawn around the edge of the tumor activity using AMIDE software (*19*). The maximum, upper 20% of voxels, and mean activities were recorded. The percentage injected dose per gram (%ID/g) and standardized uptake value (SUV) were calculated as follows: %ID/g = ROI activity ÷ injected dose × 100%. SUV = ROI activity ÷ injected dose × body weight. Spheric background ROIs with a diameter of 4 mm were drawn in homogeneous areas adjacent to the tumors to calculate tumor-to-background ratios. No partial-volume correction was applied as all tumors had size measurements > 6 mm, which was greater than 3 times the full width at half maximum resolution of the microPET scanner (*20*).

Statistical Analysis

Two-tailed Student *t* tests were performed to determine significant differences between 2 groups of data. Paired *t* tests were used when comparing changes within the same animals over time. A P value < 0.05 was chosen to indicate significance. Data were reported with standard errors of the mean.

RESULTS

CE-355621 Inhibits Tumor Xenograft Growth

Nude mice were inoculated with U87 MG human glioblastoma cells, and tumor volumes were followed for approximately 2 wk. The tumor volume growth curves for U87 MG tumor xenografts are shown in Figure 1. Compared with the baseline day 6 values, tumor growth in both the drug-treated group and the control group was significantly increased on all subsequent days after baseline. When comparing the drug-treated group with the control group, CE-355621 significantly inhibited tumor growth on day 14 (7 d after drug treatment) compared with that of the control group ($P < 0.001$). A significant difference was also found on day

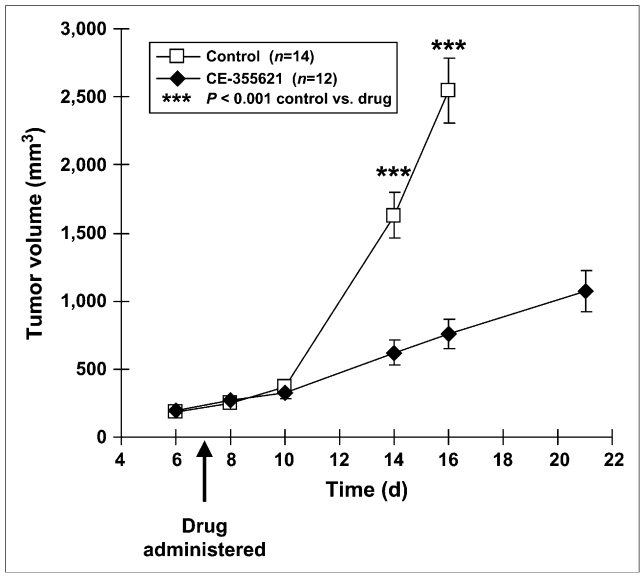

FIGURE 1. Tumor volume growth curves for U87 MG xenografts in nude mice measured by external calipers. CE-355621 or control vehicle was administered on day 7 after tumor cell inoculation. Error bars represent SEM.

16 ($P < 0.001$); however, no significant difference was seen at the earlier times points on days 8 and 10.

Mouse body weights of both groups had small increases over time. On day 16, the control group increased 8.7% compared with the day 6 baseline, whereas the drug-treated group increased 3.5%. This larger increase in the control group was significantly different ($P = 0.02$) from that of the drug-treated group on day 16 and was likely related to the differences in tumor weight between groups.

Blood glucose measurements at the time of injection ranged widely from 20 to 212 mg/dL (mean ± SD, 116 ± 47 mg/dL). There was no significant difference between the drug-treated group and the control group at each time point in the study. In addition, there was no significant difference between the pretreatment baseline values and each successive posttreatment value for the drug-treated group and the control group (Supplemental Table 1).

CE-355621 Inhibits ^{18}F-FDG Accumulation in U87 MG Xenografts

^{18}F-FDG accumulation was measured in the tumor xenografts using microPET to assess changes in the control mice (Figure 2A) compared with mice treated with CE-355621 (Fig. 2B). The maximum %ID/g of ^{18}F-FDG accumulation increased steadily over time for the control group (Fig. 3A). Each time point was significantly increased over baseline day 6, and the final maximum %ID/g on day 16 increased 66% compared with baseline. In comparison, the drug-treated group had a small increase on day 8 compared with baseline ($P = 0.008$), but days 10–22 had no significant differences compared with baseline (Fig. 3A).

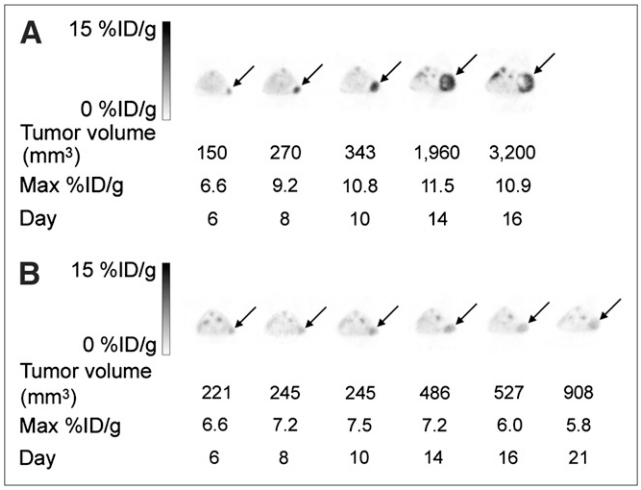

FIGURE 2. Representative axial ^{18}F-FDG microPET images from nude mice with U87 MG xenografts. Mice were scanned prone with the tumor xenograft in the right flank (arrows). Tumor volumes and maximum %ID/g are listed below the images. CE-355621 or control vehicle was administered on day 7. (A) ^{18}F-FDG accumulation increased over time in a representative control mouse xenograft. (B) ^{18}F-FDG accumulation on days 8–21 in a representative drug-treated mouse xenograft was similar to that of baseline day 6.

When comparing the drug-treated group with the control group, the maximum %ID/g of the drug-treated group was significantly less than that of the control group ($P = 0.03$) on day 10 (3 d after drug treatment). The groups remained significantly separated on days 14 and 16 ($P = 0.003$ and $P < 0.001$).

On day 8 (1 d after drug treatment), the maximum %ID/g for the drug-treated and control groups overlapped and were not significantly different ($P = 0.68$). Because the day 6 baseline values for the drug-treated group were higher than those for the control group, the data for the groups were normalized to their respective day 6 baseline values (Fig. 3B). Using the normalized data, the drug-treated group showed a nearly significant difference on day 8 (1 d after treatment) compared with that of the control group ($P = 0.06$). Thereafter, each successive time point showed a significant separation between groups ($P = 0.005$, $P = 0.002$, and $P < 0.001$).

Tumors were also analyzed using the mean %ID/g, which had some differences compared with the maximum %ID/g analysis (Fig. 4A). The control group ^{18}F-FDG accumulation peaked on day 10 and then decreased for the remaining time points. A significant difference between the drug-treated group and the control group was seen only on day 10 ($P = 0.02$). Inspection of the images revealed that control group tumors with volumes of >1,000 mm^3 had central photopenic areas consistent with tumor necrosis (Fig. 5). To compensate for the tumor necrosis, the images were reanalyzed by selecting the average activity of the hottest 20% of voxels. This reflected the most metabolically active areas of the tumor and tended to exclude the regions with tumor necrosis (Fig. 4B). The drug-treated group showed a significant difference on day 10 ($P = 0.01$), which persisted on days 14 ($P = 0.01$) and 16 ($P < 0.001$), similar to the maximum %ID/g analysis. Analysis of tumor-to-background ratios and SUVs revealed trends and significance values similar to those of the %ID/g analysis. Analysis of normalized mean %ID/g, upper 20%, tumor-to-background ratios, and SUVs also revealed similar trends and significance values.

DISCUSSION

CE-355621 is a novel antineoplastic antibody directed against the c-Met tyrosine kinase receptor. The antibody antagonizes c-Met function by blocking the binding of the ligand HGF to c-Met and by blocking ligand-dependent c-Met activation, which subsequently induces internalization and downregulation of the receptor. Several tumor cell lines express both HGF and c-Met, including the U87 MG human glioblastoma cell line (*21*). These tumor lines serve as a model to study the resulting autocrine activation of c-Met. Preliminary studies have shown that tumor growth has been inhibited in several tumor xenograft models, including U87 MG, by blocking the autocrine activation of c-Met from HGF released from the tumors (*1*). Because c-Met is upregulated in many human cancers, it is an

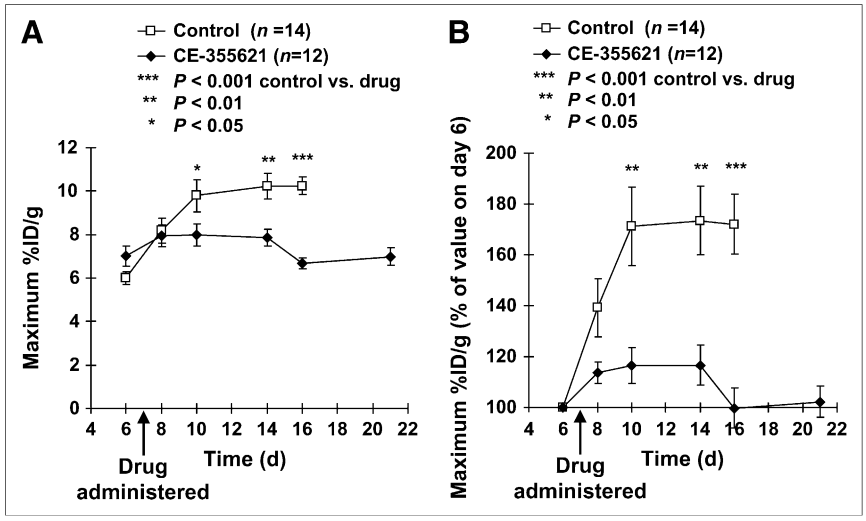

FIGURE 3. Maximum %ID/g of ^{18}F-FDG accumulation for U87 MG xenografts plotted over time. CE-355621 or control vehicle was administered on day 7. Error bars represent SEM. (A) Maximum %ID/g values are plotted. (B) Maximum %ID/g values normalized to the baseline day 6 value are plotted.

attractive novel target for cancer therapy, and its potential application has been recently reviewed by Christensen et al. (*2*).

In this study, CE-355621 significantly inhibited ^{18}F-FDG accumulation in U87 MG tumor xenografts compared with that of controls. U87 MG cells were specifically chosen to model of the c-Met/HGF autocrine loop. These findings suggest that the drug can inhibit the neoplastic process, as reflected by the downstream effect of glucose metabolism seen on ^{18}F-FDG microPET studies. No overall decrease in ^{18}F-FDG accumulation was seen in the drug-treated group compared with the baseline values; however, a targeted agent such as CE-355621 may exhibit cytostatic effects rather than cytotoxic effects, which is supported by our data. These preclinical results support the use of this novel drug in clinical trials and suggest that clinical ^{18}F-FDG PET studies may be useful to follow the early response to therapy.

Assessment of early response to therapy is desirable because it may allow early halting of ineffective treatments to avoid toxicities and allow switching to potentially effective treatments. In our study the ^{18}F-FDG accumulation curves showed a significant separation between the drug-treated group and control group 3 d after drug treatment (day 10) and a nearly significant separation 1 d after drug treatment. In comparison, separation of the tumor volume curves was seen later at 7 d after drug treatment (day 14). Early changes in ^{18}F-FDG accumulation compared with volume changes were also seen by Leyton et al., who studied the efficacy of the cytotoxic agent cisplatin in an ^{18}F-FDG microPET study (*13*). Their study showed a difference in ^{18}F-FDG accumulation between the drug-treated and control groups at 24 h, whereas a difference in tumor volume was seen later at 48 h. Several other groups (*8,10–12*) have tracked changes in tumor volume and ^{18}F-FDG accumulation; however, unlike the current study, no

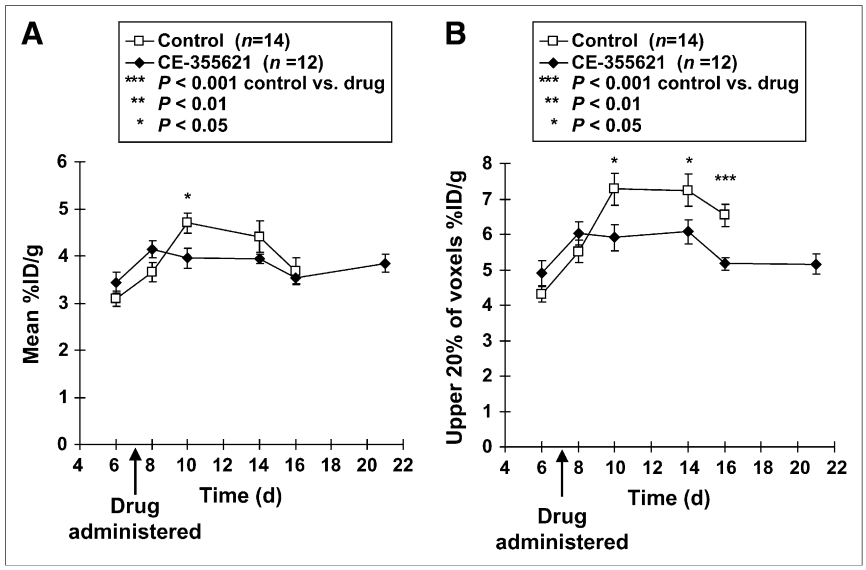

FIGURE 4. ^{18}F-FDG accumulation in U87 MG xenografts plotted over time. CE-355621 or control vehicle was administered on day 7. Error bars represent SEM. (A) Mean %ID/g values are plotted, revealing a significant separation between drug-treated group and control group only on day 10. (B) Upper 20% (of voxels) %ID/g values are plotted, revealing a significant separation on days 10, 14, and 16, similar to the maximum %ID/g values in Figure 3A.

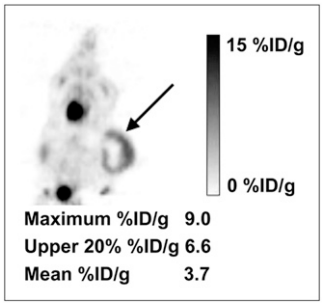

FIGURE 5. Coronal slice from a representative control group mouse with large necrotic U87 MG tumor xenograft (arrow). Central necrosis is evident as a central photopenic area. Maximum %ID/g, upper 20% (of voxels) %ID/g, and mean %ID/g are listed below the image.

direct statistical comparisons were made in any of these prior studies to assess which changes occurred earlier.

Further support for early response evaluation was shown by Cullinane et al. in a mouse xenograft ^{18}F-FDG microPET study (*6*). ^{18}F-FDG accumulation was rapidly inhibited at 4 h after treatment with the targeted receptor tyrosine kinase imatinib (Gleevac). These ^{18}F-FDG microPET findings are similar to clinical PET studies showing that decreases in ^{18}F-FDG activity preceded change in tumor size and could predict prognosis in gastrointestinal stromal tumors (*22–24*) and lymphoma (*25*). The effects seen with ^{18}F-FDG microPET in our study occurred on the time scale of days in a rapidly growing tumor xenograft model. When translating to clinical human studies, tumors are likely to exhibit slower growth, such that serial assessment will more likely be made in a time scale of weeks rather than days. Regardless of the overall time scale, we anticipate that earlier changes seen with ^{18}F-FDG PET as compared with conventional anatomic imaging (e.g., CT, MRI, and ultrasound) will significantly impact treatment decisions and survival. If tumors grow very slowly, then the effects of a cytostatic drug in an ^{18}F-FDG PET scan may not be seen for long periods of time; however, this limitation is also true for currently used anatomic imaging modalities.

An important unresolved issue is whether ^{18}F-FDG microPET results can predict the success of drugs in clinical trials. To our knowledge, the ability to prospectively predict the clinical efficacy of a novel drug using preclinical ^{18}F-FDG microPET studies has not been reported previously. If CE-355621 proceeds to clinical trials, it would be important to correlate the microPET results with ^{18}F-FDG PET studies in human trials. Preclinical animal models have had variable success in predicting clinical success (*26,27*). However, given the proven utility of ^{18}F-FDG microPET and PET for therapy monitoring, we believe that preclinical ^{18}F-FDG microPET may be a more useful predictor of the success of human clinical trials and may prove useful in accelerating drug development. These types of studies are required to assist the decision-making process of whether to proceed with a drug after preclinical animal testing. Furthermore, assessment of cytostatic targeted agents has become an important issue in clinical trials (*28*). Traditional toxicity-based endpoints may not be appropriate to evaluate the efficacy of cytostatic targeted therapies (*28,29*). Newer markers may be necessary to adequately assess phase 1 dose selection trials as well as phase 2 efficacy trials. ^{18}F-FDG PET has the potential to fulfill these roles.

An additional advantage of microPET is the ability to assess the internal metabolic characteristic of a tumor, which cannot be assessed by external caliper measurements. We found that control tumors of greater than approximately 1,000 mm^3 developed central photopenia consistent with tumor necrosis. This effect was seen by visual inspection of the images and may help explain why the maximum %ID/g continued to increase over time for the control tumors, whereas the mean %ID/g decreased. Interpretation of data from tumors with volumes $>$ 1,000 mm^3 in this xenograft model should be given with caution as tumor necrosis can have a large contribution to changes in tumor volume and mean tracer accumulation.

One limitation of our study was that we used only a single cell line in a subcutaneous mouse xenograft model that was responsive to the drug treatment. As a tumor model, subcutaneous xenografts may not be entirely representative of human disease (*26,27*). Additional studies with an orthotopic model or genetically engineered mouse models may provide additional insight into the drug's efficacy and the utility of ^{18}F-FDG microPET. In addition, studies with both chemosensitive lines as well as chemoresistant lines are needed to determine whether ^{18}F-FDG microPET can predict response to drug treatment in both types of cell lines. In clinical trials, both positive and negative results can impact the decision to proceed or terminate a drug in development. Assessing cell lines of different cancer types could also determine whether the drug is applicable across a broad range of cancers. Insights may be also obtained by assessing rapidly growing cell lines versus slowly growing cell lines. Further in vitro studies may also provide insight into the mechanism of CE-355621 on glucose metabolism as reflected by ^{18}F-FDG accumulation. Assessment with other PET tracers—such as ^{18}F-FLT for proliferation, ^{18}F-annexin-V for apoptosis, and ^{18}F-misonidazole for hypoxia—may provide additional information beyond tumor metabolism (*30,31*). Because ^{18}F-FDG may accumulate in areas of inflammation, early assessment of tumor activity may be masked by an inflammatory response to therapeutics. The use of ^{18}F-FLT may provide additional ways to assess early tumor response (*10–13,32*).

Another limitation of our study is that the ^{18}F-FDG accumulation values were not corrected for blood glucose values. Wahl et al. reported that hyperglycemia can reduce ^{18}F-FDG accumulation in rat tumors; however, other organs such as liver, spleen, heart, and muscle showed no significant difference (*33*). Recently, 2 groups have reported the effects of various anesthetic agents and fasting times in tumor-bearing mice (*34,35*). These studies highlight the complex relationship of ^{18}F-FDG accumulation, blood glucose levels, fasting state, and anesthesia. We attempted to control for these effects by using the same fasting, anesthesia, and scanning protocols for all mice. Our initial efforts to adjust ^{18}F-FDG accumulation in tumors with a glucose correction factor have not improved the accuracy of

the measurements (*15*). Further investigations into this important issue are ongoing and necessary.

CONCLUSION

CE-355621 is an efficacious novel antineoplastic agent, which inhibits ^{18}F-FDG accumulation in a mouse xenograft model compared with that of control animals. Significant inhibition of ^{18}F-FDG accumulation was seen 3 d after drug treatment, which was earlier than the inhibition of tumor volume growth seen at 7 d after drug treatment. These results encourage further testing of this novel targeted agent in clinical trials using ^{18}F-FDG PET to assess early therapy response.

ACKNOWLEDGMENTS

We thank Dr. Meike Schipper and Dr. Dirk Mayer for their technical assistance and helpful discussions. Funding was provided by Pfizer, Inc., and the NCI's Small Animal Imaging Resource Program (SAIRP grant R24CA92862).

REFERENCES

1. Michaud NR, Tsaparikos K, Hillerman S, et al. Targeting the hepatocyte growth factor receptor c-Met with neutralizing human monoclonal antibodies for the treatment of cancer. American Association of Cancer Research 97th Annual Meeting; April 1–5, 2006; Washington, D.C.
2. Christensen JG, Burrows J, Salgia R. c-Met as a target for human cancer and characterization of inhibitors for therapeutic intervention. *Cancer Lett.* 2005;225:1–26.
3. Jiang WG, Martin TA, Parr C, Davies G, Matsumoto K, Nakamura T. Hepatocyte growth factor, its receptor, and their potential value in cancer therapies. *Crit Rev Oncol Hematol.* 2005;53:35–69.
4. Gambhir SS, Czernin J, Schwimmer J, Silverman DH, Coleman RE, Phelps ME. A tabulated summary of the FDG PET literature. *J Nucl Med.* 2001;42(suppl):1S–93S.
5. Cherry SR, Shao Y, Silverman RW, et al. MicroPET: a high resolution PET scanner for imaging small animals. *IEEE Trans Nucl Sci.* 1997;44:1161–1166.
6. Cullinane C, Dorow DS, Kansara M, et al. An in vivo tumor model exploiting metabolic response as a biomarker for targeted drug development. *Cancer Res.* 2005;65:9633–9636.
7. Oyama N, Kim J, Jones LA, et al. MicroPET assessment of androgenic control of glucose and acetate uptake in the rat prostate and a prostate cancer tumor model. *Nucl Med Biol.* 2002;29:783–790.
8. Jadvar H, Xiankui L, Shahinian A, et al. Glucose metabolism of human prostate cancer mouse xenografts. *Mol Imaging.* 2005;4:91–97.
9. Su H, Bodenstein C, Dumont RA, et al. Monitoring tumor glucose utilization by positron emission tomography for the prediction of treatment response to epidermal growth factor receptor kinase inhibitors. *Clin Cancer Res.* 2006;12:5659–5667.
10. Barthel H, Cleij MC, Collingridge DR, et al. 3′-Deoxy-3′-[^{18}F]fluorothymidine as a new marker for monitoring tumor response to antiproliferative therapy in vivo with positron emission tomography. *Cancer Res.* 2003;63:3791–3798.
11. Sugiyama M, Sakahara H, Sato K, et al. Evaluation of 3′-deoxy-3′-^{18}F-fluorothymidine for monitoring tumor response to radiotherapy and photodynamic therapy in mice. *J Nucl Med.* 2004;45:1754–1758.
12. Waldherr C, Mellinghoff IK, Tran C, et al. Monitoring antiproliferative responses to kinase inhibitor therapy in mice with 3′-deoxy-3′-^{18}F-fluorothymidine PET. *J Nucl Med.* 2005;46:114–120.
13. Leyton J, Latigo JR, Perumal M, Dhaliwal H, He Q, Aboagye EO. Early detection of tumor response to chemotherapy by 3′-deoxy-3′-[^{18}F]fluorothymidine positron emission tomography: the effect of cisplatin on a fibrosarcoma tumor model in vivo. *Cancer Res.* 2005;65:4202–4210.
14. Tseng JR, Dandekar M, Subbarayan M, et al. Reproducibility of 3′-deoxy-3′-^{18}F-fluorothymidine microPET studies in tumor xenografts in mice. *J Nucl Med.* 2005;46:1851–1857.
15. Dandekar M, Tseng JR, Gambhir SS. Reproducibility of ^{18}F-FDG microPET studies in mouse tumor xenografts. *J Nucl Med.* 2007;48:602–607.
16. Ponten J, Macintyre EH. Long term culture of normal and neoplastic human glia. *Acta Pathol Microbiol Scand.* 1968;74:465–486.
17. Knoess C, Siegel S, Smith A, et al. Performance evaluation of the microPET R4 PET scanner for rodents. *Eur J Nucl Med Mol Imaging.* 2003;30:737–747.
18. Hudson HM, Larkin RS. Accelerated image reconstruction using ordered subsets of projection data. *IEEE Trans Med Imaging.* 1994;13:601–609.
19. Loening AM, Gambhir SS. AMIDE: a free software tool for multimodality medical image analysis. *Mol Imaging.* 2003;2:131–137.
20. Hoffman EJ, Huang SC, Phelps ME. Quantitation in positron emission computed tomography. 1. Effect of object size. *J Comput Assist Tomogr.* 1979;3:299–308.
21. Guerin C, Luddy C, Abounader R, Lal B, Laterra J. Glioma inhibition by HGF/NK2, an antagonist of scatter factor/hepatocyte growth factor. *Biochem Biophys Res Commun.* 2000;273:287–293.
22. Stroobants S, Goeminne J, Seegers M, et al. ^{18}FDG-Positron emission tomography for the early prediction of response in advanced soft tissue sarcoma treated with imatinib mesylate (Glivec). *Eur J Cancer.* 2003;39:2012–2020.
23. Jager PL, Gietema JA, van der Graaf WT. Imatinib mesylate for the treatment of gastrointestinal stromal tumours: best monitored with FDG PET. *Nucl Med Commun.* 2004;25:433–438.
24. Goerres GW, Stupp R, Barghouth G, et al. The value of PET, CT and in-line PET/CT in patients with gastrointestinal stromal tumours: long-term outcome of treatment with imatinib mesylate. *Eur J Nucl Med Mol Imaging.* 2005;32:153–162.
25. Jerusalem G, Hustinx R, Beguin Y, Fillet G. Evaluation of therapy for lymphoma. *Semin Nucl Med.* 2005;35:186–196.
26. Sausville EA, Burger AM. Contributions of human tumor xenografts to anticancer drug development. *Cancer Res.* 2006;66:3351–3364.
27. Becher OJ, Holland EC. Genetically engineered models have advantages over xenografts for preclinical studies. *Cancer Res.* 2006;66:3355–3358.
28. Parulekar WR, Eisenhauer EA. Phase I trial design for solid tumor studies of targeted, non-cytotoxic agents: theory and practice. *J Natl Cancer Inst.* 2004;96:990–997.
29. Fox E, Curt GA, Balis FM. Clinical trial design for target-based therapy. *Oncologist.* 2002;7:401–409.
30. Gambhir SS. Molecular imaging of cancer with positron emission tomography. *Nat Rev Cancer.* 2002;2:683–693.
31. Kelloff GJ, Krohn KA, Larson SM, et al. The progress and promise of molecular imaging probes in oncologic drug development. *Clin Cancer Res.* 2005;11:7967–7985.
32. van Waarde A, Cobben DC, Suurmeijer AJ, et al. Selectivity of ^{18}F-FLT and ^{18}F-FDG for differentiating tumor from inflammation in a rodent model. *J Nucl Med.* 2004;45:695–700.
33. Wahl RL, Henry CA, Ethier SP. Serum glucose: effects on tumor and normal tissue accumulation of 2-[F-18]-fluoro-2-deoxy-D-glucose in rodents with mammary carcinoma. *Radiology.* 1992;183:643–647.
34. Lee KH, Ko BH, Paik JY, et al. Effects of anesthetic agents and fasting duration on ^{18}F-FDG biodistribution and insulin levels in tumor-bearing mice. *J Nucl Med.* 2005;46:1531–1536.
35. Fueger BJ, Czernin J, Hildebrandt I, et al. Impact of animal handling on the results of ^{18}F-FDG PET studies in mice. *J Nucl Med.* 2006;47:999–1006.

JNM The Journal of NUCLEAR MEDICINE

Preclinical Efficacy of the c-Met Inhibitor CE-355621 in a U87 MG Mouse Xenograft Model Evaluated by ^{18}F-FDG Small-Animal PET

Jeffrey R. Tseng, Keon Wook Kang, Mangal Dandekar, Shahriar Yaghoubi, Joseph H. Lee, James G. Christensen, Stephen Muir, Patrick W. Vincent, Neil R. Michaud and Sanjiv S. Gambhir

J Nucl Med. 2008;49:129-134.
Published online: December 12, 2007.
Doi: 10.2967/jnumed.106.038836

The Journal of Nuclear Medicine is published monthly.
SNMMI | Society of Nuclear Medicine and Molecular Imaging
1850 Samuel Morse Drive, Reston, VA 20190.
(Print ISSN: 0161-5505, Online ISSN: 2159-662X)

SNMMI SOCIETY OF NUCLEAR MEDICINE AND MOLECULAR IMAGING